Contribution from the Department of Chemistry,
University of Minnesota, Minneapolis, Minnesota 55455

Synthesis and X-ray Structural Characterization of Binuclear Iridium(I) and Rhodium(I) Hydroxypyridinate Complexes. 1. Complete Assignment of the ^{1}H NMR Spectra by Two-Dimensional and NOE Techniques. The Nature of "Inside" and "Outside" ^{1}H Chemical Shift Differences

Gary S. Rodman and Kent R. Mann*

Received October 15, 1987

Six new d^8–d^8 complexes, $[Ir(COD)(\mu\text{-hp})]_2$, $[Ir(COD)(\mu\text{-mhp})]_2$, $[Ir(COD)(\mu\text{-chp})]_2$, $[Ir(COD)(\mu\text{-2hq})]_2$, $[Rh(COD)(\mu\text{-hp})]_2$, and $[Rh(COD)(\mu\text{-mhp})]_2$ (hp = 2-hydroxypyridinate, mhp = 6-methyl-2-hydroxypyridinate, chp = 6-chloro-2-hydroxypyridinate, 2hq = 2-hydroxyquinolate, COD = 1,5-cyclooctadiene), were synthesized and characterized by ^{1}H NMR, ^{13}C NMR, and IR spectroscopy and FAB mass spectrometry. Other than our preliminary communication, these are the first rhodium(I) and iridium(I) hydroxypyridinate complexes reported to date. X-ray crystallographic analyses of the isostructural $[M(COD)(\mu\text{-mhp})]_2$ (M = Ir and Rh) complexes confirmed the binuclear nature of the complexes. Both $[M(COD)(\mu\text{-mhp})]_2$ complexes crystallize in the $P2_1/c$ space group with $Z = 4$. For M = Rh, $V = 2544$ (4) Å^3, $a = 14.963$ (8) Å, $b = 12.038$ (2) Å, $c = 14.673$ (10) Å, and $\beta = 105.75$ (4)°. Full-matrix least-squares refinement (307 variables, 4006 reflections) converged to give R and R_w values of 0.028 and 0.036, respectively. For M = Ir, $V = 2521$ (4) Å^3, $a = 14.847$ (5) Å, $b = 11.991$ (2) Å, $c = 14.661$ (11) Å, and $\beta = 104.99$ (4)°. Full-matrix least-squares refinement (307 variables, 3335 reflections) converged to give R and R_w values of 0.030 and 0.031, respectively. The complexes have a "nonpolar" structure with "head-to-tail" bridging ligands that persists in solution and the gas phase. The M–M separations (Rh–Rh, 3.367 (1) Å; Ir–Ir, 3.242 (2) Å) indicate significant metal–metal interactions are present in both complexes. A twist angle (27° and 25° for M = Ir and Rh, respectively) in the flexible eight-membered $(MNCO)_2$ framework, not present in the six-membered ring of the analogous $[M(COD)(\mu\text{-pz})]_2$ (pz = pyrazolate) complexes, relieves steric strain between the two bulky COD ligands. The "open book" geometry and asymmetry of the bridging ligands attributes the molecules low-point symmetry, leading to complex NMR spectra. The complete assignment of the ^{1}H NMR spectrum of $[Ir(COD)(\mu\text{-hp})]_2$ (and by analogy, the spectra of the other five complexes) was carried out with selective decoupling, NOE, and two-dimensional NMR techniques. The NOE observed between hp proton H5 and COD proton H15 allowed the precise assignment of all 12 COD resonances. Olefinic proton H12 (trans to N and "outside") resonates downfield of olefinic proton H11 (trans to N and "inside"). Olefinic proton H15 (trans to O and "outside") resonates upfield of olefinic proton H16 (trans to O and inside). The endo methylene protons resonate upfield of the exo methylene protons. The "inside"/"outside" chemical shift differences observed for these compounds are ascribed to steric and magnetic anisotropy effects.

Introduction

We recently reported the synthesis, structural characterization, and photochemistry of $[Ir(COD)(\mu\text{-mhp})]_2$ (mhp = 6-methyl-2-hydroxypyridinate, COD = 1,5-cyclooctadiene).[1] The complete characterization of this complex is of interest because it incorporates many of the electronic structural factors we believe are needed to achieve excited-state multielectron-transfer reactions. In the present report, we discuss our results concerning the solid-, gas-, and solution-phase structures of a series of complexes of general formula $[M(COD)(\mu\text{-L})]_2$ (M = Rh, Ir; COD = 1,5-cyclooctadiene; μ-L = 2-hydroxypyridinate (μ-hp), 6-methyl-2-hydroxypyridinate (μ-mhp), 6-chloro-2-hydroxypyridinate (μ-chp), 2-hydroxyquinolate (μ-2hq)). In particular, the ^{1}H NMR, ^{13}C NMR, IR, mass spectral, and crystallographic properties of the compounds are described. The solid-state structures of $[Ir(COD)(\mu\text{-mhp})]_2$ and $[Rh(COD)(\mu\text{-mhp})]_2$ and the complete assignment of the ^{1}H and ^{13}C NMR spectra of $[M(COD)(\mu\text{-hp})]_2$ by COSY, NOE, and HETCOR techniques enable us to comment on the nature of the "inside/outside" chemical shift differences observed for these complexes. The complete assignment of the ^{1}H NMR spectra of these complexes was also necessary for the detailed elucidation of the fluxional and photochemical properties exhibited by these compounds.[2]

Experimental Section

General Information. The free ligands 2-hydroxypyridine (Hhp), 6-methyl-2-hydroxypyridine (Hmhp), 6-chloro-2-hydroxypyridine (Hchp), 2-hydroxyquinoline (H2hq), and 8-hydroxyquinoline (H8hq) were obtained from Aldrich and recrystallized from warm benzene before use, except for H8hq, which was used as received. Sodium methoxide, silver tetrafluoroborate ($AgBF_4$), and 1,5-cyclooctadiene (COD) were obtained from Aldrich and used as received. The complexes $[Ir(COD)(\mu\text{-Cl})]_2$[3] and $[Rh(COD)(\mu\text{-Cl})]_2$[4] were prepared by standard literature procedures.

Tetrahydrofuran (THF) was distilled from sodium benzophenone ketyl while acetonitrile and methylene chloride were distilled from P_4O_{10}. Reagent grade methanol was dried over activated 4-Å molecular sieves. All other solvents were reagent grade or better and used as received. Reactions involving Ir compounds were carried out under nitrogen. Elemental analyses were obtained from MHW Laboratories in Phoenix, AZ.

Instrumentation. Fast atom bombardment mass spectra (FAB-MS) were obtained on a VG Analytical VG 7070E-HF high-resolution double-focusing mass spectrometer equipped with a VG 11/250 data system. Spectra were obtained at a resolution of 1 part in 2000. Ions were generated by bombardment of the target matrix with a neutral Xe atom beam (derived from a Xe^+ ion beam accelerated at 8 KV). Samples for FAB MS were prepared by dissolution of the complexes in an *o*-nitrophenyl octyl ether matrix. Simulations of the isotopic distribution patterns were carried out by using a program provided with the VG 7070E-HF instrument.

IR spectra were obtained on Perkin-Elmer 283 (CW-IR) and Sirius 100 (FT-IR) spectrophotometers. UV–vis spectra were obtained on a Cary 17-D spectrophotometer interfaced to a Zenith 150 microcomputer.

^{1}H and ^{13}C NMR spectra were recorded at 300 and 75.5 MHz, respectively, on Nicolet NT-300 and IBM AC-300 spectrometers. Chemical shifts were referenced to the residual proton or carbon signals of the solvent. The following values were used: ^{1}H NMR, δ 7.26 for $CDCl_3$, 7.15 for C_6D_6, and 2.09 for the methyl resonance of toluene-d_8; ^{13}C NMR, δ 77.0 for $CDCl_3$, 128.0 for C_6D_6, and 20.4 for the methyl resonance of toluene-d_8. All shifts are reported in units of δ.

COSY spectra were obtained on the AC-300 instrument by using 256 individual scans with eight acquisitions per scan. ^{1}H–^{13}C correlated (HETCOR) spectra were obtained on the AC-300 instrument by using 128 individual scans with 32 or 64 acquisitions per spectrum. Selective decoupling and NOE experiments were carried out on the NT-300 instrument. For selective decoupling, a decoupling power of 45 dB was used. For NOE experiments, a particular resonance was presaturated for 3 s with a decoupling power of 35 dB, and the FID was acquired with the decoupler off. NOE was observed by subtracting each irradiated spectrum from a reference spectrum (obtained by irradiation of an empty region in the compound's spectrum). Typically, 80 acquisitions per spectrum were used.

* To whom correspondence should be addressed.

(1) Rodman, G. S.; Mann, K. R. *Inorg. Chem.* **1985**, *24*, 3507.
(2) Rodman, G. S.; Daws, C. A.; Mann, K. R. *Inorg. Chem.*, in press.
(3) Herde, J. L.; Lambert, J. C.; Senoff, C. V. *Inorg. Synth.* **1974**, *15*, 18.
(4) Chatt, J. C.; Venanzi, L. M. *J. Chem. Soc.* **1957**, 4735.

0020-1669/88/1327-3338$01.50/0

NMR samples were prepared by the vacuum transfer of degassed (four freeze–pump–thaw cycles) deuteriated solvent into evacuated tubes that contained the solid compound. The tubes were then sealed off under vacuum with a torch.

NMR simulations were carried out an Zenith 150 microcomputer with the RACCOON[5] program and on the NT-300 with a program supplied with the instrument. Simulation of COD olefin resonances was carried out in two parts of five spins each. Simulation of COD methylene resonances was carried out in two parts of six spins each. Trial values of chemical shifts and coupling constants were obtained from selective decoupling experiments.

Preparation of Compounds. Hydroxypyridinate Salts. Sodium salts of the hydroxypyridine ligands were prepared by the reaction of the desired compound with 1 equiv of sodium methoxide in dry methanol.

[Ir(COD)(μ-hp)]$_2$. [Ir(COD)(μ-Cl)]$_2$ (501 mg, 0.821 mmol) and Na(hp) (192 mg, 1.64 mmol) were added to a 100-mL Schlenk flask equipped with a magnetic stir bar. The flask was stoppered and purged with N_2, and then 15 mL of degassed THF was added via syringe. The deep red solution was stirred at room temperature for 2.5 h and then taken to dryness. The product was extracted into THF (15 mL) and filtered through a short column of diatomaceous earth. The compound was crystallized by addition of CH_3CN (75 mL), filtered, and dried under vacuum overnight, giving 547 mg of [Ir(COD)(μ-hp)]$_2$ as dull red microcrystals. The yield was 85% based on Ir. ^{1}H NMR (300 MHz, $CDCl_3$, 25 °C): hp, 7.92 (m, 1 H), 7.07 (m, 1 H), 6.34 (m, 1 H), 6.24 (m, 1 H); COD, 4.63 (m, 1 H), 4.42 (m, 1 H), 3.56 (m, 1 H), 2.87 (m, 1 H), 2.74 (m, 1 H), 2.52 (m, 2 H), 2.12 (m, 1 H), 1.84 (m, 1 H), 1.73 (m, 1 H), 1.44 (m, 1 H), 1.32 (m, 1 H). ^{13}C{^{1}H} NMR (75.5 MHz, C_6D_6, 25 °C): hp, 179.14, 147.66, 137.11, 117.12, 112.94; COD, 75.35, 60.56, 57.55, 52.94, 34.43, 33.10, 31.26, 30.14. λ_{max} = 490 nm; ϵ_{max} = 4.7 × 10^3 M^{-1} cm^{-1}. Anal. Calcd for $Ir_2C_{26}H_{32}N_2O_2$: C, 39.58; H, 4.09; N, 3.55. Found: C, 39.67; H, 4.47; N, 3.64.

[Ir(COD)(μ-mhp)]$_2$. The preparation was similar to that of [Ir(COD)(μ-hp)]$_2$, except that methylene chloride was substituted for THF. Starting with 511 mg (0.760 mmol) of [Ir(COD)(μ-Cl)]$_2$ and 254 mg (1.940 mmol) of Na(mhp) gave 446 mg of [Ir(COD)(μ-mhp)]$_2$ as red-orange microcrystals. The yield was 72% based on Ir. ^{1}H NMR (300 MHz, $CDCl_3$, 25 °C): mhp, 7.02 (t, 1 H), 6.16 (t, 2 H), 2.80 (s, 3 H); COD, 4.65 (m, 1 H), 4.26 (m, 1 H), 3.73 (m, 1 H), 2.67 (m, 1 H), 2.61 (m, 1 H), 2.48 (m, 2 H), 2.10 (m, 1 H), 1.69 (m, 2 H), 1.41 (m, 1 H), 1.26 (m, 1 H). ^{13}C{^{1}H} NMR (75.5 MHz, $CDCl_3$, 25 °C): mhp, 173.30, 154.83, 138.03, 113.60, 112.96, 23.81; COD, 72.62, 57.58, 55.37, 54.31, 33.49, 32.29, 30.50, 29.41. λ_{max} = 484 nm; ϵ_{max} = 4.6 × 10^3 M^{-1} cm^{-1}. Anal. Calcd for $Ir_2C_{28}H_{36}N_2O_2$: C, 41.16; H, 4.44; N, 3.43. Found: C, 41.13; H, 4.70; N, 3.56.

[Ir(COD)(μ-chp)]$_2$. The preparation was similar to that of [Ir(COD)(μ-hp)]$_2$. Starting with 265 mg (0.394 mmol) of [Ir(COD)(μ-Cl)]$_2$ and 119.3 mg (0.787 mmol) of Na(chp) gave 260 mg of [Ir(COD)(μ-chp)]$_2$ as an orange powder. The yield was 89% based on Ir. ^{1}H NMR (300 MHz, $CDCl_3$, 25 °C): chp, 7.10 (m, 1 H), 6.36 (m, 2 H); COD: 4.71 (m, 1 H), 4.30 (m, 1 H), 3.68 (m, 1 H), 2.87 (m, 1 H), 2.71 (m, 1 H), 2.50 (m, 2 H), 2.17 (m, 1 H), 1.73 (m, 2 H), 1.48 (m, 1 H), 1.26 (m, 1 H). ^{13}C{^{1}H} NMR (75.5 MHz, $CDCl_3$, 25 °C): chp, 174.23, 145.89, 139.10, 119.48, 113.17; COD, 72.83, 57.62, 56.31, 54.36, 33.33, 31.95, 30.51, 29.61. λ_{max} = 490 nm; ϵ_{max} = 5.1 × 10^3 M^{-1} cm^{-1}. Anal. Calcd for $Ir_2C_{26}H_{30}Cl_2N_2O_2$: C, 36.40; H, 3.52; N, 3.26. Found: C, 36.57; H, 3.79; N, 3.14.

[Ir(COD)(μ-2hq)]$_2$. The preparation was similar to that of [Ir(COD)(μ-hp)]$_2$, except that methylene chloride was substituted for THF. Starting with 511.0 mg (0.761 mmol) of [Ir(COD)(μ-Cl)]$_2$ and 283 mg (1.696 mmol) of Na(2hq) gave 282 mg of [Ir(COD)(μ-2hq)]$_2$ as a red powder. The yield was 42% based on Ir. ^{1}H NMR (300 MHz, $CDCl_3$, 25 °C): 2hq, 9.480 (m, 1 H), 7.568 (m, 1 H), 7.229 (m, 2 H), 7.096 (m, 1 H), 6.292 (d, 1 H); COD, 4.851 (m, 1 H), 4.508 (m, 1 H), 3.746 (m, 1 H), 2.76 (m, 2 H), 2.63 (m, 2 H), 2.10 (m, 1 H), 1.62 (m, 3 H), 1.3 (m, 1 H). ^{13}C{^{1}H} NMR (75.5 MHz, $CDCl_3$, 25 °C): 2hq, 173.10, 145.48, 137.33, 128.28, 126.94, 124.12, 123.92, 122.46, 118.94; COD, 72.83, 58.97, 57.21, 54.52, 33.32, 32.17, 30.84, 29.97. λ_{max} = 499 nm; ϵ_{max} = 3.2 × 10^3 M^{-1} cm^{-1}. Anal. Calcd for $Ir_2C_{34}H_{36}N_2O_2$: C, 45.93; H, 4.08; N, 3.15. Found: C, 45.82; H, 4.28; N, 3.07.

Ir(COD)(8hq).[6] The preparation was similar to that of [Ir(COD)(μ-hp)]$_2$. Starting with 305 mg (0.453 mmol) of [Ir(COD)(μ-Cl)]$_2$ and 152 mg (0.907 mmol) of Na(8hq) gave 370 mg of [Ir(COD)(8hq)] as deep red microcrystals. The yield was 92% based on Ir. ^{1}H NMR (C_6D_6, 25 °C): 8hq, 7.43 (m, 2 H), 7.30 (m, 2 H), 6.62 (dd, 1 H), 6.38 (dd, 1 H); COD, 4.93 (br, 2 H), 3.56 (br, 2 H), 2.26 (br, 4 H), 1.67 (br m, 4 H). ^{13}C{^{1}H} NMR (C_6D_6, 25 °C): 8hq, 172.0, 144.54, 138.76, 131.40, 130.74, 120.32, 115.66, 112.37; COD, 69.38, 52.00, 31.86, 31.51.

[Rh(COD)(μ-hp)]$_2$. The Rh_2 complexes were prepared from [Rh(COD)(CH_3CN)$_2$][BF_4]. [Rh(COD)(μ-Cl)]$_2$ (348 mg, 0.706 mmol) and $AgBF_4$ (275 mg, 1.41 mmol) were placed in a 100-mL beaker equipped with a magnetic stir bar. Acetonitrile (25 mL) was added, and the yellow solution was stirred for 15 min, during which time AgCl precipitated. The solution of [Rh(COD)(CH_3CN)$_2$][BF_4] was filtered through medium-grade filter paper, and Na(hp) (166 mg, 1.41 mmol) was added. This solution was stirred overnight during which time a yellow precipitate formed. The solution was taken to dryness, and the product was extracted into benzene (40 mL). The $NaBF_4$ was filtered away on a fine frit, and the benzene was removed to give the product as a bright yellow powder, which was recrystallized from CH_2Cl_2/CH_3CN. The yield was 250 mg (58% based on Rh). ^{1}H NMR (300 MHz, toluene-d_8, −53 °C): hp, 8.202 (d, 1 H), 6.576 (t, 1 H), 6.469 (d, 1 H), 5.880 (t, 1 H); COD: 5.385 (m, 1 H), 5.109 (m, 1 H), 4.120 (m, 1 H), 3.292 (m, 1 H), 3.125 (m, 1 H), 2.775 (m, 1 H), 2.617 (m, 1 H), 2.06 (m, 1 H), 1.95 (m, 2 H), 1.610 (m, 1 H), 1.410 (m, 1 H). ^{13}C{^{1}H} NMR (75.5 MHz, toluene-d_8, −53 °C): hp, 175.32, 147.78, 136.86, 116.48, 111.25; COD, 76 (d), 60.0 (d), 58.0 (d), 53.0 (d), 35.0, 33.0, 30.1, 29.0. λ_{max} = 422 nm; ϵ_{max} = 3.0 × 10^3 M^{-1} cm^{-1}. Anal. Calcd for $Rh_2C_{26}H_{32}N_2O_2$: C, 51.16; H, 5.28; N, 4.59. Found: C, 50.84; H, 5.39; N, 4.44.

[Rh(COD)(μ-mhp)]$_2$. The preparation was similar to that of [Rh(COD)(μ-hp)]$_2$. Starting with 328 mg (0.664 mmol) of [Rh(COD)(μ-Cl)]$_2$, 310 mg (1.60 mmol) of $AgBF_4$, and 175 mg (1.34 mmol) of Na(mhp) gave 299 mg of [Rh(COD)(μ-mhp)]$_2$ as a bright yellow powder. The yield of the mhp complex was 70% based on Rh. ^{1}H NMR (300 MHz, toluene-d_8, −53 °C): mhp, 6.683 (t, 1 H), 6.292 (d, 1 H), 5.848 (d, 1 H), 3.085 (s, 3 H); COD, 5.334 (m, 1 H), 5.041 (m, 1 H), 4.277 (m, 1 H), 3.1 (m, 1 H), 2.683 (m, 2 H), 2.050 (m, 1 H), 1.88 (m, 2 H), 1.643 (m, 1 H), 1.340 (m, 1 H). ^{13}C{^{1}H} NMR (75.5 MHz, toluene-d_8, −53 °C): mhp, 174.9, 155.3, 137.9, 112.5, 111.8, 29.9; COD, 88.2 (d), 76.2 (d), 72.4 (d), 72.2 (d), 33.4, 32.1, 30.5, 29.2. λ_{max} = 420 nm; ϵ_{max} = 2.8 × 10^3 M^{-1} cm^{-1}. Anal. Calcd for $Rh_2C_{28}H_{36}N_2O_2$: C, 52.68; H, 5.68; N, 4.39. Found: C, 52.45; H, 5.94; N, 4.51.

Rh(COD)(8hq).[7] The preparation was similar to that of [Rh(COD)(μ-hp)]$_2$. Starting with 223 mg (0.452 mmol) of [Rh(COD)(μ-Cl)]$_2$, 176 mg (0.905 mmol) of $AgBF_4$, and 151 mg (0.905 mmol) of Na(8hq) gave 199 mg of [Rh(COD)(8hq)] as an orange powder. The yield was 62% based on Rh. ^{1}H NMR (C_6D_6, 25 °C): 8hq, 7.461 (dd, 1 H), 7.294 (m, 2 H), 7.084 (d, 1 H), 6.672 (dd, 1 H), 6.406 (dd, 1 H); COD, 5.00 (br, 2 H), 3.69 (br, 2 H), 2.28 (br m, 4 H), 1.71 (br m, 4 H).

Solution Molecular Weight Determination of [Ir(COD)(μ-mhp)]$_2$. The molecular weight of [Ir(COD)(μ-mhp)]$_2$ in methylene chloride was determined by the Signer method of isothermal distillation.[8] The molecular weight was determined to be 990 ± 200 with Cp_2Fe as the reference compound. The calculated molecular weight based on the binuclear formulation is 817.04.

Collection and Reduction of Crystallographic Data. Crystals of [Ir(COD)(μ-mhp)]$_2$ and [Rh(COD)(μ-mhp)]$_2$ were obtained by carefully layering degassed CH_3CN onto CH_2Cl_2 solutions of the complexes. A well-formed crystal of each compound was mounted in air on a glass fiber for structure determination.

Data were collected on a Enraf-Nonius SPD-CAD4 automatic diffractometer,[9] and the automatic peak searching, centering, and indexing routines and calculations were performed on PDP8A and 11/34 computers as described previously.[9] Crystal data and collection parameters are given in Table I. Crystal decomposition was monitored by three check reflections taken prior to data collection and after every 100 min of exposure time. No decay or significant fluctuation was observed during data collection for the Ir_2 compound. A 1.3% decay in intensity of the check reflections was observed during data collection for the Rh_2 compound, and a linear correction was applied. Scattering factors were taken from Cromer and Waber,[10] and the effects of anomalous dispersion were included.[11] Empirical absorption corrections were made based on φ scans with χ near 90°.

The structures were solved from the three-dimensional Patterson map, which allowed placement of the metal atoms. Fourier and difference

(5) Schatz, P. F. Program written for IBM PC microcomputers.
(6) Uson, R.; Oro, L. A.; Ciriano, M. A.; Gonzales, R. J. *J. Organomet. Chem.* **1981**, *205*, 259.
(7) Ugo, R.; La Monica, G.; Cenini, S.; Bonati, F. *J. Organomet. Chem.* **1968**, *11*, 159.
(8) Signer, R. *Justus Liebig. Ann. Chem.* **1930**, *478*, 246.
(9) McNair, A. M.; Boyd, D. C.; Mann, K. R. *Organometallics* **1986**, *5*, 303.
(10) Cromer, D. T.; Waber, J. T. *International Tables for X-Ray Crystallography*; Kynoch: Birmingham, England, 1974; Vol. IV, Table 2.2.4. Cromer, D. T. *Ibid.*, Table 2.3.1.
(11) Cromer, D. T.; Ibers, J. A. *International Tables for X-Ray Crystallography*; Kynoch: Birmingham, England, 1974; Vol. IV.

Table I. Crystallographic Data and Collection Parameters for $[Ir(COD)(\mu\text{-mhp})]_2$ and $[Rh(COD)(\mu\text{-mhp})]_2$

formula	$Ir_2C_{28}H_{36}N_2O_2$	$Rh_2C_{28}H_{36}N_2O_2$
M_r	817.04	638.41
cryst syst	monoclinic	monoclinic
space group	$P2_1/c$	$P2_1/c$
a, Å	14.847 (5)	14.963 (8)
b, Å	11.991 (2)	12.038 (2)
c, Å	14.661 (11)	14.673 (10)
α, deg	90.04 (4)	89.98 (4)
β, deg	104.99 (4)	105.75 (4)
γ, deg	89.99 (2)	90.00 (3)
cell vol, Å^3	2521	2544
Z	4	4
d(calcd), g cm^{-3}	2.152	1.667
cryst dimens, mm	0.15 × 0.20 × 0.20	0.20 × 0.25 × 0.30
μ, cm^{-1}	105.40	13.04
empirical abs cor	0.829–1.000	0.805–1.000
diffractometer	CAD 4	CAD 4
radiation	Mo Kα (λ = 0.71073 Å)	Mo Kα (λ = 0.71073 Å)
scan type	ω–2θ	ω–2θ
2θ range, deg	0–50	0–50
tot. no. of reflcns	4437	4988
no. of reflcns with $F_o^2 > \sigma(F_o^2)$	3335	4006
no. of variables	307	307
P	0.030	0.030
std dev of observn of unit wt	1.22	1.53
R	0.0295	0.0281
R_w	0.0313	0.0360

Fourier analysis in conjunction with cycles of least-squares refinement allowed placement of the remaining atoms, excluding the hydrogens. Full-matrix least-squares refinement utilized anisotropic temperature factors for all non-hydrogen atoms (307 variables). Hydrogens (except for those on the methyl groups) were placed at idealized positions, given β values of 5.0, and not refined.

The final difference Fourier map of the Ir_2 structure revealed 10 "ghost" peaks of 0.77–0.97 e/Å^3, all less than 1.4 Å from an Ir atom. The final difference Fourier map of the Rh_2 structure revealed no significant features except those due to residual electron density of the methyl hydrogens. These were not included in any of the calculations. Tables II and III contain the final positional parameters for $[Ir(COD)(\mu\text{-mhp})]_2$ and $[Rh(COD)(\mu\text{-mhp})]_2$, respectively.[12]

Results and Discussion

Syntheses. The preparations of the new hydroxypyridinate-bridged compounds $[Ir(COD)(\mu\text{-L})]_2$ are straightforward and proceed smoothly with isolated yields of between 40 and 90%. The compounds are air stable in the solid state but decompose over several hours in aerated solutions. The yields depended on the solubility of the complexes in the THF/CH_3CN or CH_2Cl_2/CH_3CN solvent combinations used to crystallize the compounds. The procedures are chloride metathesis reactions, where the bridging chlorides in $[Ir(COD)(\mu\text{-Cl})]_2$ are displaced by a hydroxypyridinate (or hydroxyquinolinate) anion. Such metathetical reactions are well-known for $[Ir(COD)(\mu\text{-Cl})]_2$,[13] as this was the method employed by Stobart and co-workers to prepare $[Ir(COD)(\mu\text{-pz})]_2$[14] (pz = pyrazolate). A mononuclear complex ([Ir(COD)(8hq)]) (8hq = 8-hydroxyquinolate) prepared by a similar method,[6] was useful as a model for the assignment of the NMR spectra of the binuclear species.

The air-stable Rh_2 analogues were synthesized from the acetonitrile complex $[Rh(COD)(CH_3CN)_2][BF_4]$. Isolated yields ranged between 60 and 70%. As in the synthesis of the Ir analogues, some product was inevitably left in solution, and no attempts to isolate second crops were carried out. The mononuclear model complex analogous to [Ir(COD)(8hq)], [Rh(COD)(8hq)], has been previously prepared.[7]

(12) See the supplementary material for the calculated positional and thermal parameters for the H atoms, anisotropic thermal parameters for non-H atoms, and calculated and observed structure factors.
(13) Leigh, G. J.; Richards, R. L. In *Comprehensive Organometallic Chemistry*; Wilkinson, G., Stone, F. G. A., Abel, E. W., Eds.; Pergamon: Oxford, England, 1982; Vol. V.
(14) Coleman, A. W.; Eadie, D. T.; Stobart, S. R.; Zaworotko, M. J.; Atwood, J. L. *J. Am. Chem. Soc.* **1982**, *104*, 922.

Table II. Positional Parameters and Their Estimated Standard Deviations for $[Ir(COD)(\mu\text{-mhp})]_2$

atom	x	y	z
Ir1	0.20564 (2)	0.10784 (3)	0.15308 (2)
Ir2	0.35186 (2)	0.26632 (3)	0.08349 (2)
N1A	0.2817 (4)	0.3779 (5)	0.1546 (4)
O1A	0.2640 (4)	0.2316 (4)	0.2485 (3)
C1A	0.2550 (5)	0.3372 (6)	0.2306 (5)
C2A	0.2218 (6)	0.4088 (7)	0.2893 (5)
C3A	0.2088 (6)	0.5178 (7)	0.2662 (6)
C4A	0.2319 (6)	0.5582 (7)	0.1860 (6)
C5A	0.2677 (5)	0.4890 (6)	0.1317 (5)
C6A	0.2922 (6)	0.5275 (7)	0.0432 (6)
N1B	0.1181 (4)	0.2270 (5)	0.0644 (4)
O1B	0.2288 (3)	0.2353 (5)	−0.0170 (3)
C1B	0.1482 (5)	0.2656 (6)	−0.0077 (5)
C2B	0.0908 (6)	0.3375 (7)	−0.0745 (6)
C3B	0.0073 (6)	0.3712 (7)	−0.0626 (7)
C4B	−0.0215 (6)	0.3332 (8)	0.0138 (7)
C5B	0.0336 (5)	0.2602 (7)	0.0768 (6)
C6B	0.0066 (7)	0.2210 (9)	0.1630 (7)
C11C	0.3082 (6)	−0.0091 (7)	0.2180 (6)
C12C	0.2423 (6)	0.0004 (7)	0.2693 (6)
C13C	0.1668 (7)	−0.0849 (8)	0.2685 (7)
C14C	0.1059 (8)	−0.1089 (9)	0.1714 (8)
C15C	0.1088 (6)	−0.0185 (7)	0.0998 (6)
C16C	0.1759 (7)	−0.0153 (7)	0.0466 (6)
C17C	0.2526 (7)	−0.0989 (7)	0.0558 (7)
C18C	0.3153 (8)	−0.1068 (9)	0.1554 (7)
C11D	0.4216 (5)	0.1345 (7)	0.0352 (6)
C12D	0.4197 (6)	0.2281 (8)	−0.0220 (6)
C13D	0.5007 (7)	0.3035 (9)	−0.0185 (6)
C14D	0.5451 (6)	0.3455 (9)	0.0823 (6)
C15D	0.4790 (6)	0.3468 (8)	0.1437 (6)
C16D	0.4680 (6)	0.2554 (8)	0.1993 (6)
C17D	0.5215 (6)	0.1485 (9)	0.2020 (7)
C18D	0.5083 (7)	0.0958 (8)	0.1054 (8)

Table III. Positional Parameters and Their Estimated Standard Deviations for $[Rh(COD)(\mu\text{-mhp})]_2$

atom	x	y	z
Rh1	0.20354 (2)	0.10233 (2)	0.15228 (2)
Rh2	0.35538 (2)	0.26625 (2)	0.08317 (2)
N1A	0.2842 (2)	0.3760 (2)	0.1540 (2)
O1A	0.2696 (2)	0.2267 (2)	0.2449 (2)
C1A	0.2572 (2)	0.3316 (3)	0.2273 (2)
C2A	0.2196 (3)	0.4001 (3)	0.2846 (3)
C3A	0.2050 (3)	0.5093 (4)	0.2626 (3)
C4A	0.2275 (3)	0.5525 (3)	0.1841 (3)
C5A	0.2672 (2)	0.4854 (3)	0.1309 (2)
C6A	0.2925 (3)	0.5275 (4)	0.0450 (3)
N1B	0.1174 (2)	0.2224 (2)	0.0638 (2)
O1B	0.2303 (2)	0.2253 (2)	−0.0131 (2)
C1B	0.1505 (2)	0.2604 (3)	−0.0077 (2)
C2B	0.0978 (3)	0.3343 (3)	−0.0742 (3)
C3B	0.0145 (3)	0.3714 (4)	−0.0646 (3)
C4B	−0.0166 (3)	0.3359 (4)	0.0095 (3)
C5B	0.0345 (3)	0.2611 (3)	0.0738 (3)
C6B	0.0050 (3)	0.2201 (5)	0.1579 (3)
C11C	0.3067 (3)	−0.0148 (3)	0.2153 (3)
C12C	0.2449 (3)	−0.0050 (3)	0.2687 (3)
C13C	0.1696 (4)	−0.0884 (4)	0.2699 (4)
C14C	0.1074 (4)	−0.1122 (4)	0.1730 (4)
C15C	0.1057 (3)	−0.0241 (4)	0.1011 (3)
C16C	0.1670 (3)	−0.0196 (3)	0.0470 (3)
C17C	0.2447 (4)	−0.1022 (4)	0.0528 (4)
C18C	0.3105 (4)	−0.1118 (4)	0.1506 (4)
C11D	0.4246 (3)	0.1339 (4)	0.0349 (3)
C12D	0.4208 (3)	0.2250 (4)	−0.0229 (3)
C13D	0.4995 (3)	0.3026 (5)	−0.0196 (3)
C14D	0.5455 (3)	0.3455 (4)	0.0792 (3)
C15D	0.4823 (2)	0.3467 (4)	0.1422 (3)
C16D	0.4732 (3)	0.2602 (4)	0.1997 (3)
C17D	0.5238 (3)	0.1531 (4)	0.2047 (4)
C18D	0.5120 (3)	0.0983 (4)	0.1089 (4)

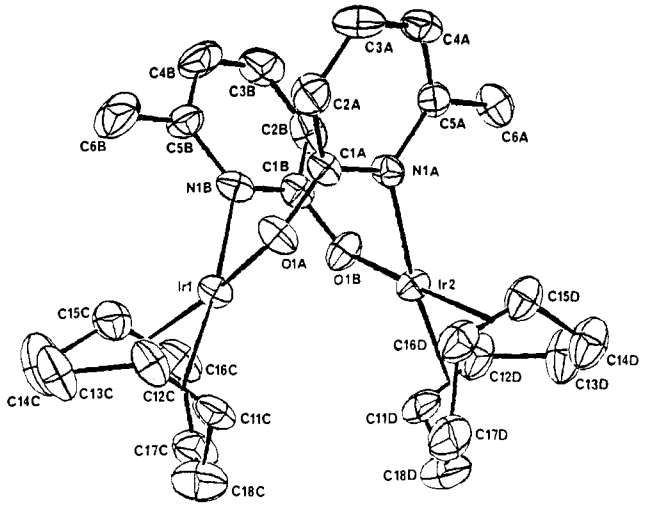

Figure 1. Crystal structure of $[Ir(COD)(\mu\text{-mhp})]_2$. Thermal elipsoids are drawn at the 50% probability level.

The binuclear nature of the $[M(COD)(\mu\text{-L})]_2$ complexes was indicated by FAB mass spectra, a solution molecular weight determination, and IR spectral data.[15] The complexes exhibit parent ion multiplets in the FAB mass spectra in excellent agreement with their calculated isotopic distributions. The solution molecular weight determination of $[Ir(COD)(\mu\text{-mhp})]_2$ by the Signer method[8] was in good agreement with the binuclear formulation. IR spectral data indicate that the solution spectra of all the compounds studied are virtually identical with the spectra obtained in KBr pellets. Finally, the successful assignment and simulation of the ^1H NMR spectra of these compounds (vide infra) indicates that in each case the solution species has a structure very similar to that of the crystalline material.

Structural Characterization. Solid-State Structures of $[Ir(COD)(\mu\text{-mhp})]_2$ and $[Rh(COD)(\mu\text{-mhp})]_2$. The compounds $[Ir(COD)(\mu\text{-mhp})]_2$ and $[Rh(COD)(\mu\text{-mhp})]_2$ both crystallize in the $P2_1/c$ space group, with $Z = 4$, and are isostructural. An ORTEP view of $[Ir(COD)(\mu\text{-mhp})]_2$ with the atomic labeling scheme is shown in Figure 1. Important bond distances and angles are given in Table IV. Complete structural data are given in the supplementary material.

The molecules have approximate C_2 symmetry, with pseudo-C_2 axes between the two mhp ligands bisecting the M–M vectors. The complexes are chiral, but both enantiomers are present in the unit cell. The dissymmetry of $[M(COD)(\mu\text{-mhp})]_2$ is similar to that of $[Ir(PPh_3)(CO)(\mu\text{-pz})]_2$,[16] where the chirality is caused by the arrangement of two different terminal ligands at each Ir.

The coordination sphere at each M(I) center is made up of a chelating η^4-COD ligand and a pyridine nitrogen from one and a pyridinolate oxygen from the other bridging mhp group. The eight-membered $(MNCO)_2$ ring adopts a twisted "tub" conformation that gives M–M distances of 3.242 (1) and 3.367 (1) Å for $[Ir(COD)(\mu\text{-mhp})]_2$ and $[Rh(COD)(\mu\text{-mhp})]_2$, respectively. These values fall within the range of distances found in other weakly interacting d^8–d^8 systems. For example, in two prototypical complexes of this type, $[Rh_2(bridge)_4]^{2+}$ (bridge = 1,3-diisocyanopropane) (face-to-face geometry)[17] and $[Ir(COD)(\mu\text{-pz})]_2$ (open-book geometry),[14,18] the M–M separations are 3.246 (1) and 3.216 (1) Å, respectively. Interestingly, the 0.125-Å increase in M–M separation between $[Ir(COD)(\mu\text{-mhp})]_2$ and $[Rh(COD)(\mu\text{-mhp})]_2$ is much larger than the 0.051-Å difference seen between the Ir pyrazolyl-bridged complex and its Rh analogue.[18]

Table IV. Selected Average Bond Distances (Å) and Angles (deg) in $[M(COD)(\mu\text{-mhp})]_2$[a]

	M = Ir	M = Rh
Distances		
Coordination Core		
M1–M2	3.242 (2)	3.267 (1)
M–N	2.103 (8)	2.132 (3)
M–O	2.066 (6)	2.079 (3)
M–S12	1.986 (15)	1.996 (6)
M–S56	1.977 (15)	1.984 (6)
M–C11	2.109 (10)	2.109 (10)
M–C12	2.097 (11)	2.097 (11)
M–C15	2.098 (11)	2.098 (11)
M–C16	2.099 (11)	2.099 (11)
mhp Ligands		
C–O	1.292 (12)	1.290 (5)
C–N	1.362 (17)	1.362 (8)
C–C (ring)	1.376 (30)	1.376 (13)
C–C	1.509 (41)	1.506 (18)
COD Ligands		
C=C (trans to N)	1.390 (16)	1.375 (7)
C=C (trans to O)	1.409 (16)	1.369 (7)
C—C	1.509 (41)	1.506 (18)
Angles		
O–M–N	90.6 (3)	90.4 (2)
O–M–S12	89.1 (6)	89.1 (2)
N–M–S56	91.5 (6)	92.0 (2)
S12–M–S56	88.0 (6)	88.2 (2)
M–N–C1	116.6 (6)	115.2 (3)
M–N–C5	123.4 (7)	124.8 (3)
M–O–C	123.6 (6)	123.8 (3)

[a] Standard deviations calculated as $(\sum \sigma_i^2)^{1/2}$.

Table V. Close Nonbonding Distances (Å) in $[M(COD)(\mu\text{-mhp})]_2$[a]

	M = Ir	M = Rh
COD(D)–COD(D)		
H11C–H17D	2.07	2.13
H16C–H11D	2.73	2.99
H17C–H11D	2.17	2.27
H18C–H18D	2.45	2.59
mhp–COD (Closest Approach)		
H6A–H15D	1.88	1.86
H6B–H15C	1.80	1.77

[a] Assumes C–H = 1.07 Å.

This effect is ascribed to a greater flexibility of the $(MNCO)_2$ bridging framework relative to the $(MNN)_2$ found in bis(pyrazolyl-bridged) complexes.[19]

The hydroxypyridinate ligand can bring two metal centers into close proximity as evidenced by the structure of $Cr_2(\mu\text{-mhp})_4$, which contains an "exceedingly short" Cr–Cr quadruple bond[20] of 1.889 (1) Å. A more relevant example is the d^8–d^8 complex $[Pt(NH_3)_2(\mu\text{-hp})]_2^{2+}$, which has a Pt–Pt separation of only 2.898 Å.[21] We believe much of the 0.35 Å difference in M–M distance between this Pt_2 complex and $[Ir(COD)(\mu\text{-mhp})]_2$ is due to steric repulsions between the COD ligands in the latter molecule (vide infra). The important interactions are listed in Table V. In particular, the calculated distances for H11C–H17D and H11D–H17C are significantly shorter than the sum of the van der Waals radii of two hydrogen atoms (2.4 Å).[22] In an analogous compound, $[Rh(NBD)(\mu\text{-chp})]_2$, which employs the less sterically

(15) IR spectral data are included as Supplementary Table S7.
(16) Beveridge, K. A.; Bushnell, G. W.; Dixon, K. R.; Eadie, D. T.; Stobart, S. R.; Atwood, J. L.; Zaworothko, M. J. *J. Am. Chem. Soc.* **1982**, *104*, 920.
(17) Mann, K. R.; Thich, J. A.; Bell, R. A.; Coyle, C. L.; Gray, H. B. *Inorg. Chem.* **1980**, *19*, 2462.
(18) Beveridge, K. A.; Bushnell, G. W.; Stobart, S. R.; Atwood, J. L.; Zaworothko, M. J. *Organometallics* **1983**, *2*, 1447.
(19) The pyrazolyl ligand is capable of accommodating a variety of M–M separations when the other ligands are allowed to change. For example, $(Et_3P)_2Pt(\mu\text{-pz})_2Cr(CO)_4$ (Stobart, S. R.; Dixon, K. R.; Eadie, D. T.; Atwood, J. L.; Zaworothko, M. J. *Angew. Chem., Int. Ed. Engl.* **1980**, *19*, 931) has a M–M distance of 3.683 (3) Å and $[Ir_2(COD)_2(pz)_2(\mu\text{-}C_4F_6)]$ has a M–M distance of 2.623 (2) Å.[16]
(20) Cotton, F. A.; Fenwick, P. E.; Niswander, R. H.; Sekutowski, J. C. *J. Am. Chem. Soc.* **1978**, *100*, 4725.
(21) Hollis, L. S.; Lippard, S. J. *J. Am. Chem. Soc.* **1983**, *105*, 3494.
(22) Weast, R. C., Ed. *CRC Handbook of Chemistry and Physics*, 58th ed.; CRC: Cleveland, OH, 1978; p D-178.

demanding norbornadiene (NBD) ligand, a Rh–Rh separation of 3.040 (1) Å has been achieved.[23]

The relative orientation of the two M(I) square planes in each compound is significantly different from either the face-to-face geometry common for d^8–d^8 complexes containing four bridging ligands or the open-book orientation found in $[Ir(COD)(\mu\text{-pz})]_2$. The dihedral angles between the square planes are 56 and 57° for $[Ir(COD)(\mu\text{-mhp})]_2$ and $[Rh(COD)(\mu\text{-mhp})]_2$, respectively, and both structures exhibit a twist about the metal–metal vector away from the eclipsed conformation. This twist angle is evaluated as the dihedral angle p1–M1–M2–p2, where p1 and p2 are the centroids of the four olefinic carbons (C11C, C12C, C15C, and C16C and C11D, C12D, C15D, and C16D, respectively). The twist angles are 27° and 25° for $[Ir(COD)(\mu\text{-mhp})]_2$ and $[Rh(COD)(\mu\text{-mhp})]_2$, respectively. While these dihedral and twist angles sharply contrast the analogous parameters in $[M(COD)(\mu\text{-pz})]_2$, in which the dihedral angles are some 17° larger (78.5°, M = Ir; 80.7, M = Rh),[18] and the planes are perfectly eclipsed (twist angle = 0°), comparable dihedral and twist angles are reported for the complex $[Rh(NBD)(\mu\text{-OAc})]_2$ (dihedral angle = 50.10, twist angle = 25°).[24] It is reasonable to assume that the twist observed in the structures of $[Ir(COD)(\mu\text{-mhp})]_2$ and $[Rh(COD)(\mu\text{-mhp})]_2$ lessens the unfavorable steric interaction between the COD ligands.

Each metal center in both complexes exhibits almost perfect square-planar geometry, as shown by the planes calculated for M1, N1B, O1A, S12C, and S56C and M2, N1A, O1B, S12D, and S56D (S12 and S56 are the centers of the C11–C12 and C15–C16 bonds, respectively). The average M–N distances are almost identical in the two complexes, 2.130 (8) (M = Ir) and 2.132 (3) Å (M = Rh), while the average M–O distances are slightly shorter in the Ir complex: 2.066 (6) Å (M = Ir) and 2.079 (3) Å (M = Rh). The Rh–N distances are ca. 0.07 Å longer and the Rh–O distances are ca. 0.05 Å longer than the same distances in $Rh_2(mhp)_4$,[25] consistent with the higher metal oxidation state in the tetrakis compound. The average M–S12 and M–S56 distances are identical within 2 standard deviations for each molecule; the data are not sufficient to distinguish a structural trans influence between mhp N and O in these compounds. All coordination sphere bond angles for both complexes are close to 90°.

The COD ligands adopt the usual "tub" conformation in both compounds. The four olefinic carbon atoms of each COD ligand are nearly coplanar. The average C=C bond lengths are 1.390 (16) (trans to N) and 1.409 (16) Å (trans to O) for M = Ir. The C=C bonds are somewhat shorter in the Rh compound (1.375 (7) (trans to N) and 1.369 (7) Å (trans to O)), consistent with a higher degree of metal to ligand π-back-bonding for the more electron-rich Ir(I) metal centers. The slightly shorter C=C distances compared to the analogous distances in $[M(COD)(pz)]_2$ (1.41 (2) Å for M = Ir and 1.39 (2) Å for M = Rh)[18] suggest the mhp ligand is a weaker σ donor (or less likely, a better π acceptor) than pz. The average C–C bond is 1.51 Å in both compounds, with no appreciable difference between sp^2–sp^3 and sp^3–sp^3 single-bond lengths.

The mhp ligands are essentially planar, except for slight deviations observed for the oxygen and methyl carbon atoms. For M = Ir, the average deviations from the mhp planes are 0.061 Å for O1 and 0.056 Å for C6. For M = Rh, the corresponding deviations are 0.059 Å and 0.041 Å for O1 and C6, respectively. The M(I) atoms are not coplanar with the mhp ligands. In the Ir_2 complex, the average distance between the Ir atoms and the N-bound mhp plane is 0.204 Å, while the analogous distance in the Rh_2 complex is 0.154 Å. In both complexes the internal and exocyclic bond angles of the mhp heterocycles are within experimental error of 120°, as are the O1–C1–N1 and O1–C1–C2 angles. Slightly larger deviations from 120° are seen in the angles involving the M atoms, which are in the range 116–124° (M = Ir) and 115–125° (M = Rh). The corresponding angles in face-to-face Rh(II)-Rh(II) complexes containing four mhp ligands are between 118 and 120°.[25]

Table VI. ^1H NMR Parameters for $[Ir(COD)(\mu\text{-hp})]_2$ in $CDCl_3$

atom	chem shift, δ	coupled protons	protons enhanced by NOE[a]
H2	6.34 (d)	H3	H3
H3	7.07 (t of d)	H2, H4, H5	H2, H4, H5(–)
H4	6.24 (t of d)	H3, H5	H2(–), H3, H5
H5	7.92 (d of d)	H3, H4	H3(–), H4, H15
H11	4.42 (t of d)	H12, H18, H18′	H12, H15, H16
H12	4.63 (t)	H11, H13	H11, H13
H13	2.50 (m)	H12, H13′, H14, H14′	
H13′	1.84 (m)	H13, H14, H14′	
H14	2.12 (m)	H13, H13′, H14′, H15	
H14′	1.32 (m)	H13, H13′, H14, H15	
H15	2.87 (t of d)	H14, H14′, H16	H5, H11, H16
H16	3.56 (t)	H15, H17	H11, H15
H17	2.74 (m)	H16, H17′, H18, H18′	
H17′	1.73 (m)	H17, H18, H18′	
H18	2.55 (m)	H11, H17, H17′, H18′	
H18′	1.44 (m)	H11, H17, H18, H17′	

[a] At 250 K. Minus sign denotes negative enhancements.

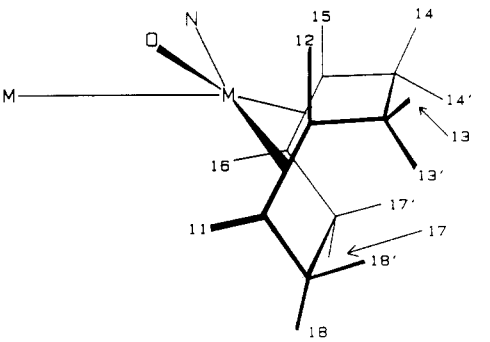

Figure 2. η^4-COD labeling scheme for NMR discussion. Olefinic hydrogens are 11, 12, 15, and 16. Methylene hydrogens are 13, 13′, 14, 14′, 17, and 17′. Hydrogens 11, 16, 17, 17′, 18, and 18′ are "inside" while 12, 15, 13, 13′, 14, and 14′ are "outside" with respect to the distal metal. Methylene hydrogens labeled with a prime are endo (13′, 14′, 17′, 18′) while 13, 14, 17, and 18 are exo.

Assignment of the ^1H NMR Spectra. The ^1H NMR spectra (COD region) of all the hydroxypyridinate complexes studied are very similar, but low temperatures are required to obtain sharp spectra for the Rh compounds.[26] We present a detailed discussion only for $[Ir(COD)(\mu\text{-hp})]_2$. The ^1H NMR data for this complex are summarized in Table VI.

Table VII lists the coupling constants derived from the simulation of the COD region of the spectrum.[27] Figure 2 shows the labeling scheme used throughout the NMR discussion. Figure 3 shows the COD region of the COSY spectrum.

The ^1H NMR spectrum of each hydroxypyridinate complex shows a total of 12 different COD resonances (some of which overlap). The number of resonances is *only* consistent with the binuclear solid-state structures in which both COD ligands are chemically equivalent, but each proton of a given COD is chemically distinct due to the low symmetry of the complexes. A monomeric species with a chelating hydroxypyridinate ligand would have C_s symmetry and give rise to a maximum of six resonances. The COSY spectrum unequivocally rules out a "polar", "head-to-head" isomer containing nonequivalent COD ligands. While the "polar" geometry would also produce 12 COD resonances, the connectivity indicated by the COSY spectrum indicates that all 12 resonances are connected by coupling, consistent *only* with the "head-to-tail" solution structure.

(23) Boyd, D. C. Ph.D. Thesis, University of Minnesota, 1987.
(24) Reis, A. H., Jr.; Willi, C.; Siegel, S.; Tani, B. *Inorg. Chem.* **1979**, *18*, 1859.
(25) Cotton, F. A.; Felthouse, T. R. *Inorg. Chem.* **1981**, *20*, 584.
(26) At 298 K, the Rh_2 complexes are fluxional on the NMR time scale.
(27) Supplementary Figure S1 illustrates the simulated and experimental COD region of the ^1H NMR spectrum of $[Ir(COD)(\mu\text{-hp})]_2$.

Table VII. Coupling Constants (Hz) from the Simulation of the ^{1}H NMR Spectrum of $[Ir(COD)(\mu\text{-hp})]_2$

	H12 1	H11 2	H16 3	H15 4	H17 5	H18 6	H13 7	H14 8	H13′ 9	H17′ 10	H18′ 11	H14′ 12
H12	1	7.25	0.00	0.00	0.00	0.00	7.10	0.00	0.00	0.00	0.00	0.00
H11	2		0.00	0.00	0.00	7.55	0.00	0.00	0.00	0.00	4.44	0.00
H16	3			7.16	7.40	0.00	0.00	0.00	0.00	0.00	0.00	0.00
H15	4				0.00	0.00	0.00	8.00	0.00	0.00	0.00	4.38
H17	5					12.00	0.00	0.00	0.00	9.00	9.10	0.00
H18	6						0.00	0.00	0.00	6.00	13.00	0.00
H13	7							11.50	9.50	0.00	0.00	8.50
H14	8								5.10	0.00	0.00	13.80
H13′	9									0.00	0.00	8.60
H17′	10										8.60	0.00
H18′	11											0.00
H14′	12											

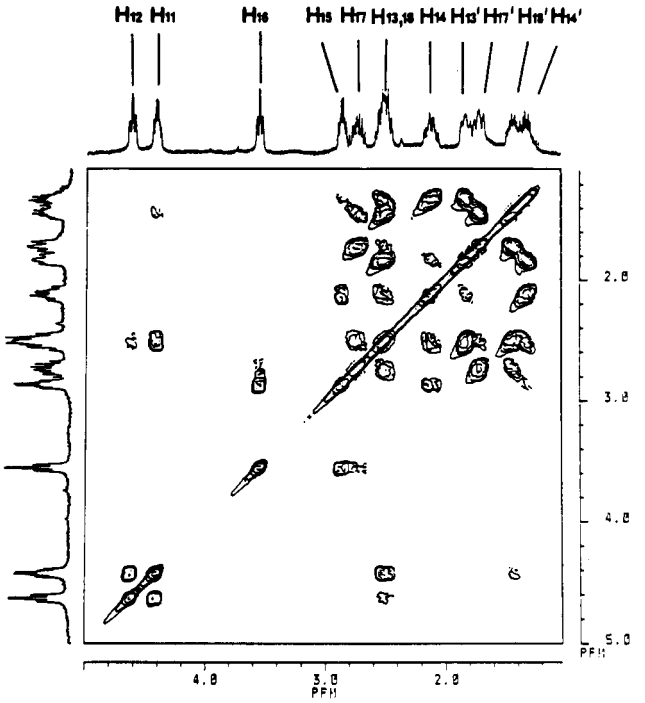

Figure 3. COSY spectrum of $[Ir(COD)(\mu\text{-hp})]_2$, COD region.

Assignment of the μ-hp Region. The hp protons are labeled H2, H3, H4, and H5. The unambiguous assignment of the resonance due to H5 in $[Ir(COD)(\mu\text{-hp})]_2$ was crucial to the correct assignment of the COD protons. Protons H2 and H5 were expected to give essentially doublet resonances, with the more downfield doublet at 7.92 ppm assigned to H5, because it is adjacent to the pyridine N. Further support for this assignment comes from an examination of the spectra of the 6-position-substituted mhp and chp complexes, which lack the 7.92 ppm resonance. The doublet at 6.34 ppm in the hp complex is, therefore, due to H2. In a decoupling experiment, the irradiation of resonance H5 collapses the triplet of doublets at 6.24 ppm into a doublet and the triplet of doublets at 7.07 ppm into a triplet. The 6.24 ppm resonance is due to H4, and the 7.07 ppm resonance is due to H3, based on the relative magnitudes of the their coupling constants to H5 (J^4(H3–H5) = 0.7 Hz, J^3(H4–H5) = 7.5 Hz). These assignments[28] are consistent with the NOE data. The observed negative NOE between the resonances due to H3 and H5 and H2 and H4 is characteristic of "linear" three-spin systems. In these systems, negative enhancements occur when the second spin away from the saturated spin is observed.[29] This type of negative enhancement has been observed previously in other aromatic systems.[29]

(28) The ^{1}H spectrum of the protonated, free Hhp ligand has been assigned previously: Aksnes, D. W.; Kryvi, H. *Acta Chem. Scand.* **1972**, *26*, 2255.

(29) Noggle, J. H.; Schreimer, R. E. *The Nuclear Overhauser Effect*; Academic: New York, 1971.

Table VIII. ^{1}H NMR Data (δ) for Rh(I) and Ir(I) COD Complexes in the Olefin Region (in $CDCl_3$ Unless Noted)

	trans to N		trans to O	
	outside[c]	inside[d]	inside[e]	outside[f]
$[Ir(COD)(\mu\text{-hp})]_2$	4.63	4.42	3.56	2.87
$[Ir(COD)(\mu\text{-mhp})]_2$	4.65	4.25	3.72	2.61
$[Ir(COD)(\mu\text{-chp})]_2$	4.71	4.30	3.68	2.87
$[Ir(COD)(\mu\text{-2hq})]_2$	4.85	4.51	3.75	2.79
$[Rh(COD)(\mu\text{-hp})]_2$[a]	5.38	5.11	4.12	3.29
$[Rh(COD)(\mu\text{-mhp})]_2$[a]	5.33	5.04	4.28	2.91
[Ir(COD)(8hq)][b]	4.93		3.56	
[Rh(COD)(8hq)][b]	5.00		3.69	
[Ir(COD)(sal=NR)]				
R = CH_3	4.4		3.6	
R = C_6H_{11}	4.4		3.4	
R = C_6H_5	4.4		3.0	
[Rh(COD)(sal=NR)]				
R = CH_3	4.6		3.8	
R = C_6H_{11}	4.6		3.6	
R = C_6H_5	4.6		3.2	
$[Ir(COD)(\mu\text{-pz})]_2$[a]	4.00	3.45		
$[Ir(COD)(\mu\text{-OAc})]_2$			4.09[g]	3.88[g]

[a] Toluene-d_8 at 220 K. [b] Benzene-d_6. [c] Resonance due to H12. [d] Resonance due to H11. [e] Resonance due to H16. [f] Resonance due to H15. [g] Assigned here based on hydroxypyridinate complexes.

Assignment of the COD Region. The four most downfield resonances in the COD region are assigned to the olefinic protons (labeled H11, H12, H15, and H16), based on the spectra of other Ir(I) COD complexes (see Table VIII) and on the relatively simple coupling patterns of these signals. There are 24 possible assignments for these four resonances, and the correct assignment could not be unambiguously made from model compounds or chemical intuition. Sixteen of the assignments are eliminated through the selective decoupling of each olefinic proton signal. These experiments indicate the resonances at 4.42 and 4.63 ppm are from protons sharing one double bond, while those at 2.87 and 3.56 ppm share the other double bond. The COSY spectrum (Figure 3) shows no other olefinic proton–olefinic proton coupling. Coupling between olefinic protons on different double bonds through the Ir center is unlikely to account for the observed ca. 7 hz coupling constants; this was verified by the observed absence of coupling between olefin protons trans to N and trans to O in [Ir(COD)(8hq)].

There are eight possible assignments remaining. In an unsuccessful attempt to decide which pairs of signals are from protons trans to N and which are from those trans to O, the NMR spectra of various relevant Rh(I) and Ir(I) olefin complexes were considered (Table VIII). Several monomeric Ir(I) COD complexes with chelating ligands have been prepared, including [Ir(COD)(8hq)][6] and a variety of Schiff's base complexes.[30] In every case, there are two olefinic proton resonances, one due to two equivalent protons on double bonds trans to N and one due to those trans to O. The upfield resonance in each compound occurs

(30) (a) Platzer, N.; Goasdove, N.; Bonnaire, R. *J. Organomet. Chem.* **1976**, *104*, 107. (b) Cozens, R. J.; Murray, K. S.; West, B. O. *Ibid.* **1971**, *27*, 399.

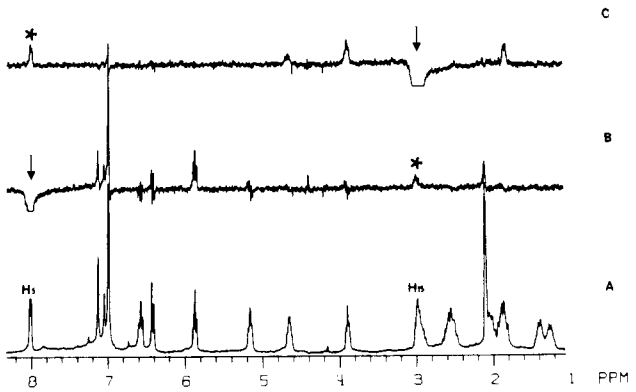

Figure 4. NOE experiments with $[Ir(COD)(\mu\text{-hp})]_2$: (A) reference spectrum; (B) difference spectrum obtained upon irradiation of H5 resonance (indicated by arrow) where the starred peak is the enhanced olefinic resonance; (C) difference spectrum obtained upon irradiation of H15 resonance (indicated by arrow), where the starred peak is the enhanced hp resonance.

between 3.0 and 3.6 ppm, while the downfield resonance occurs between 4.4 and 5.0 ppm. There has been some debate in the literature regarding the assignment of the NMR signals. For example, Uson et al.[6] assigned the downfield resonance (4.93 ppm) of [Ir(COD)(8hq)] to the protons trans to O, while Ugo et al.[7] assigned the downfield resonance (5.00 ppm) of the Rh analogue to the protons trans to N. Similar ambiguity is seen in the assignment of Schiff base complexes containing olefin ligands. Kriz and Bouchal[31] assigned the downfield protons resonances in $[Rh(C_2H_4)_2(sal{=}NR)]$ (where sal=N = *o*-O—C_6H_5—CH=N—R with R = CH_3 or C_6H_5) to the trans to O protons. However, Bonnaire et al.[30a] made the opposite assignment for [M(COD)(sal=NR)], M = Rh and Ir. Although Bonnaire's assignment, based on steric and ring current effect arguments, was convincing, it was uncertain whether identical arguments would apply to the binuclear hydroxypyridinate compounds studied here. Additionally, the spectra of binuclear "model" compounds $[Ir(COD)(\mu\text{-pz})]_2$ and $[Ir(COD)(\mu\text{-OAc})]_2$, which only have protons trans to only one type of atom, are of little help in this regard. It was clear that a technique independent of chemical shift was necessary to unambiguously discern the olefinic protons trans to N from those trans to O. The nuclear Overhauser effect (NOE) was such a technique.

The X-ray crystal structure of $[Ir(COD)(\mu\text{-mhp})]_2$ shows that the methyl group of the bridging mhp ligand is much closer to olefinic proton H15 than to the other three olefinic protons. The minimum calculated distance between a methyl proton and H15 is 1.8 Å compared with 4.2 Å to the next nearest olefinic proton. This suggested that the strong distance dependence of the nuclear Overhauser effect could be used to distinguish the resonance due to H15. The unambiguous assignment of *one* of the COD resonances allows for the assignment of *every* COD resonance with the COSY and selective decoupling data. However, because the methyl proton resonance chemical shift is so close to one of the olefinic proton resonances, the NOE study of $[Ir(COD)(\mu\text{-mhp})]_2$ itself was not conclusive. For this reason, the unsubstituted $[Ir(COD)(\mu\text{-hp})]_2$ complex was studied, with definitive results.

Figure 4 shows the results of NOE experiments carried out for $[Ir(COD)(\mu\text{-hp})]_2$ at 251 K in toluene-d_8. The NOE study was carried out at a low temperature (250 K) to eliminate the negative enhancements due to the chemical exchange processes that occur at higher temperatures. Irradiation of the H5 resonance at 7.92 ppm (Figure 4B) enhances the olefinic proton resonance at 2.87 ppm, the only COD signal to be enhanced. (In toluene-d_8, this resonance slightly overlaps a methylene proton signal.) Conversely, irradiation of the resonance at 2.87 ppm (Figure 4C) enhances the H5 resonance, the only hp resonance to be enhanced. The enhancement factor is 11.5% based on peak area. There is no appreciable NOE between between any other COD–hp resonance pair. The 2.87 ppm triplet is assigned to H15. Although a crystal structure of $[Ir(COD)(\mu\text{-hp})]_2$ is not available, the calculated distance between hp proton H5 and COD proton H15 is 2.5 Å, based on the structure of the mhp analogue, with the next nearest olefinic proton 4.2 Å away.

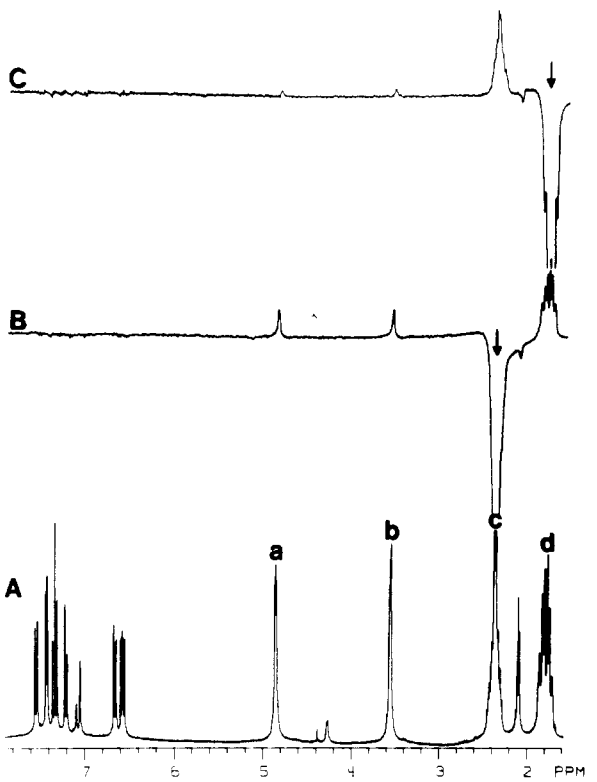

Figure 5. NOE experiments with [Ir(COD)(8hq)]: (A) reference spectrum; (B) difference spectrum obtained upon irradiation of methylene resonance C; (C) difference spectrum obtained upon irradiation of methylene resonance D. In each case, the arrow indicates the irradiated resonance.

The remaining 11 signals are assigned with the aid of the COSY spectrum, coupling constants from simulations, and the use of model compounds. But first it was necessary to differentiate exo (labeled H13, H14, H17, and H18) from endo (labeled H13′, H14′, H17′, and H18′) methylene proton resonances (endo protons are labeled with primes). The calculated values of the olefinic–methylene vicinal coupling constants (with a modified Karplus equation[32] appropriate to organic molecules with dihedral angles derived from crystallographic data) did not agree with the simulated values and so were of no use in this regard. NOE experiments could in principle distinguish exo from endo methylene proton resonances (for example, H15 is closer to H14 than H14′ by 0.57 Å in $[Ir(COD)(\mu\text{-mhp})]_2$) but unfortunately, there is no discernible NOE between olefinic and methylene protons in the hydroxypyridinate compounds. NOE is observed between olefinic and methylene COD resonances in COD complexes of higher symmetry. Figure 5 displays the results of NOE experiments performed on [Ir(COD)(8hq)]. Resonances A and B are due to the olefinic protons, while resonances C and D are due to the methylene protons. Irradiation of resonance C leads to strong and equal enhancements of both resonances A and B, while irradiation of resonance D gives weak and equal enhancement of resonance A and B. The results of these experiments unambiguously show that resonance C is due to the exo methylene protons. (Apparently trans to N and trans to O methylene protons have very similar chemical shifts.) This result is apparently constant

(31) Kriz, J.; Bouchal, K. *J. Organomet. Chem.* **1974**, *64*, 255.

(32) (a) Gunther, H. *NMR Spectroscopy*; Wiley: New York, 1980. (b) Calculated and observed vicinal coupling are in Supplementary Table S8. (c) The allylic coupling constants were calculated by using the following equations: $^3J = 6.6\cos^2\phi + 2.6\sin^2\phi$ ($0° \le \phi \le 90°$); $^3J = 11.6\cos^2\phi + 2.6\sin^2\phi$ ($90° \le \phi \le 180°$). Garbisch, E. W., Jr. *J. Am. Chem. Soc.* **1964**, *86*, 5561.

from complex to complex as our results for the symmetrically bridged binuclear complex $[Ir(COD)(\mu\text{-pz})]_2$, the results of Cramer, for ethylene complexes,[33] and the assignment for $[Rh(COD)(\mu\text{-pz})]_2$[34] are in accord. With the consistency of these results, whenever there was a choice in assignment between endo and exo methylene protons, the more downfield signal was assigned to the exo protons.

The H15 resonance couples to responances at 3.56, 2.12, and 1.32 ppm, with coupling constants of 7.16, 8.00, and 4.38 Hz, respectively. The signal at 3.56 ppm is due to an olefinic proton, and must be assigned to H16. The other signals are due to methylene protons three bonds away from H15, because the magnitude of the coupling is too large for four-bond coupling. The 2.12 ppm resonance is due to (the exo) H14 and the 1.32 ppm resonance is due to (the endo) H14′, based on the above chemical shift argument. In addition to coupling to H15 and H14′, the H14 signal couples to the resonance at 1.84 ppm (J = 5.1 Hz) and one of two overlapping signals at 2.45–2.60 ppm (11.5 Hz). The 1.84 ppm signal is due to H13′, but neither the selective decoupling nor COSY data is sufficient to resolve the overlapping multiplets. In all solvents that spectra were obtained in ($CDCl_3$, C_6D_6, toluene-d_8), the two methylene signals overlap. The assignment of H13 to the resonance simulated at 2.50 ppm is based on the COSY spectrum of $[Ir(COD)(\mu\text{-mhp})]_2$ (see supplementary material) in which the analogous multiplets are more resolved (the coupling pattern is quite similar).

Next, H16 couples to the resonance at 2.74 ppm (J = 7.40 hz), which is assigned to H17. H17 is coupled to resonances at 1.73 (J = 9.00 Hz) and 1.44 ppm (J = 9.10 Hz) and one of the multiplets at 2.45–2.60 ppm (J = 12.00 Hz). The olefinic resonance at 4.42 ppm (either H11 or H12) also couples to the methylene resonances at 1.44 ppm and 2.45–2.60 ppm, with coupling constants of 4.44 and 7.5 Hz, respectively. Again the magnitudes of the observed couplings preclude four-bond coupling and require the 1.44 and 2.45–2.60 ppm resonances to reside on the same carbon atom. The methylene signals are, therefore, assigned to H18′ (1.44 ppm) and H18 (simulated value = 2.55 ppm). The remaining methylene resonance at 1.73 ppm is assigned to H17′, and the olefinic signals at 4.42 ppm and 4.63 ppm are assigned with confidence to H11 and H12. It is important to note that the crucial olefinic proton assignments do not depend on the resolution of the two methylene multiplet signals that fall between 2.45 and 2.60 ppm. No assignment scheme other than the one shown in Table VI is consistent with the selective decoupling, COSY, and NOE data.

^{13}C NMR Spectra. The ^{13}C NMR spectrum of $[Ir(COD)(\mu\text{-hp})]_2$ was assigned (with the exception of the methylene resonances) by ^1H–^{13}C correlated 2-D spectroscopy (HETCOR). The other complexes gave similar HETCOR spectra, so the assignments are identical. Table IX summarizes assignments of the olafinic COD ^{13}C resonances for the hydroxypyridinate compounds. The position of the ^{13}C resonances are consistent with the ^{13}C NMR spectra of the compounds [Ir(COD)(8hq)], $[Ir(COD)(\mu\text{-pz})]_2$, and $[Ir(COD)(\mu\text{-OAc})]_2$. The data indicate that olefinic carbons trans to N are more deshielded that those trans to O. Because of the large difference in chemical shift between exo and endo protons, the signal due to each methylene C–H correlation is half that of an olefinic C–H correlation and is not distinguishable from the noise background. Thus, it was not possible to assign the methylene region.

The relative ^{13}C and ^1H chemical shifts for the hp ligand are parallel, but the relative chemical shifts of the carbon resonances of the COD olefinic carbons are quite different from the relative shifts of the olefinic proton resonances. In particular, there is a large difference in chemical shift for the carbons trans to N than for those trans to O. This result is the opposite of that observed for the olefinic proton resonances. Additionally, while the H15 resonance occurs downfield of the H16 resonance, the resonance due to C15 is upfield of the C16 resonance.

Table IX. ^{13}C NMR Spectral Data (δ) for Hydroxypyridinate Complexes in the COD Olefinic Region

	trans to N		trans to O	
	outside[d]	inside[e]	outside[f]	inside[g]
$[Ir(COD)(\mu\text{-hp})]_2$[a]	72.29	60.52	57.50	52.88
$[Ir(COD)(\mu\text{-mhp})]_2$[b]	73.09	57.59	55.37	54.49
$[Ir(COD)(\mu\text{-chp})]_2$[c]	72.82	57.62	56.31	54.36
$[Ir(COD)(\mu\text{-2hq})]_2$[c]	72.83	58.97	57.21	54.52
$[Rh(COD)(\mu\text{-hp})]_2$[b] (220 K)	89.13	77.23	74.41	70.96
$[Rh(COD)(\mu\text{-mhp})]_2$[b] (220 K)	87.69	76.56	72.83	72.21
$[Ir(COD)(\mu\text{-pz})]_2$[b]	68.59[h]	65.64[h]		
$[Ir(COD)(OAc)]_2$[b]			63.66[h]	55.48[h]
[Ir(COD)(8hq)][a]	69.39		52.00	
[Rh(COD)(8hq)][c]	84.28		70.40	

[a] C_6D_6. [b] Toluene. [c] $CDCl_3$. [d] Resonance due to C12. [e] Resonance due to C11. [f] Resonance due to C15. [g] Resonance due to C16. [h] Our assignment based on hydroxypyridinate complexes.

Generalization of the ^1H NMR Assignment. The generalization of the detailed ^1H NMR assignment should be of use in the assignment of the spectra of other COD complexes of similar geometry. For a given C=C bond, we find that one olefinic proton resonance is an approximate triplet, while the other is an approximate triplet of doublets. For the pair of olefinic protons trans to N, H12 (the "outside" proton) gives the simpler pattern, while for the pair protons trans to O, it is H16 (the "inside" olefinic proton) that displays the simpler pattern. The vicinal (allylic) coupling constants calculated from the standard organic chemistry model,[32] and the appropriate dihedral angles derived from the crystal structure of $[Ir(COD)(\mu\text{-mhp})]_2$ are in poor agreement with the observed coupling pattern. However, the trends in the observed vicinal couplings for H12 and H16 and H11 and H15 are consistent with the crystallographic dihedral angles.[35]

Our assignment of the COD region of the hydroxypyridinate complexes is consistent with those previous assignments of the olefinic protons trans to a pyridine nitrogen deshielded relative to olefinic protons trans to a phenolate oxygen. Perhaps most importantly, our data indicate that the direction of the chemical shift has no predictive value in the assignments of "inside" olefinic protons (ie. H11 and H16) and "outside" olefinic protons (ie. H12 and H15) in "open-book" complexes.[36] The inside/outside shift is in the opposite direction for olefinic protons trans to N and trans to O.

What Causes the "Inside/Outside" Chemical Shift? A discussion of the cause of the large chemical shift differences seen in both ^1H and ^{13}C NMR spectra of COD atoms trans to the same atom but with either the "outside" or "inside" orientation is in order. Simple arguments based on electronegativity of substituents, heavy-atom effects, conjugation, excited-state mixing, and the like are unable to explain the observed chemical shift differences because the "inside/outside" chemical shift results from the geometry of the $[M(COD)(\mu\text{-L})]_2$ complexes.

Two different geometric effects are relevant in the $[M(COD)(\mu\text{-L})]_2$ complexes: steric crowding that results in hybridization changes at carbon and concomitant changes in both ^{13}C and ^1H chemical shifts and magnetic anisotropy. Two sources of steric crowding are present in the $[M(COD)(\mu\text{-L})]_2$ complexes: (1) the short distance between H15 (the proton trans to oxygen and "outside") and the bridging ligands, and (2) the steric crowding between the bulky COD ligands. Table V lists the

(33) (a) Cramer, R. *J. Am. Chem. Soc.* **1964**, *86*, 217. (b) Cramer, R. *Ibid.* **1969**, *91*, 2519.

(34) Elguero, J.; Esteban, M.; Grenier-Loustalot, M. F.; Oro, L. A.; Pinillos, M. T. *J. Chim. Phys. Phys.-Chim. Biol.* **1984**, *81*, 251.

(35) It is not surprising that the standard parameters used in the Karplus type equations to calculate vicinal coupling constants for free olefins are quite inappropriate for use in olefin complexes, because, in addition to the dihedral angle, the magnitude of vicinal coupling is sensitive to C–C bond length, H–C–C bond angle, and substituent electronegativity,[38] all of which are altered upon coordination.

(36) In conjunction with the studies carried out for the hydroxypyridinate complexes, an NOE study of $[Ir(COD)(\mu\text{-pz})]_2$ was undertaken. The downfield olefinic proton resonance (4.00 ppm in toluene-d_8) is due to the "outside" olefinic protons. For details, see: Rodman, G. S. Ph.D. Thesis, 1987, University of Minnesota.

structurally significant close nonbonding distances. It is difficult to evaluate quantitatively the individual contributions to the observed chemical shift differences; however, some qualitative comments can be made.

As is shown in Table VIII, the chemical shift difference between the H15 and H16 (the trans to O outside and inside entries, respectively) resonances increases with substitution of the C5 position of the bridging hydroxypyridinate ligand. The mhp complex gives the largest shift difference of 1.11 ppm compared to a difference of 0.70 ppm for the unsubstituted hp complex, with the chp and 2hq complexes giving intermediate values of 0.81 and 0.96 ppm, respectively. Most of the *variation* in chemical shift difference between the H15 and H16 resonances is accounted for by shifts of the H15 signal. Steric considerations predict H15 to be most affected by changes in the bridging ligand.

A similar steric interaction was postulated to account for the observance of two resonances for olefinic protons and carbons trans to O in the complex [Ir(COD)(Sal-*o*-tol)].[37a] A crystal structure of this molecule indicates that the *o*-tolyl group is oriented perpendicular to the Ir(I) square plane,[37b] so that only one end of the double bond trans to oxygen interacts with the tolyl methyl group. In contrast, a single resonance was observed for the olefinic carbons and protons trans to N. In the binuclear complexes considered here, the short distance between H16 on one COD and H11 on the other COD is an additional steric effect, presumably similar in magnitude in all the hydroxypyridinate complexes studied here.

The chemical shift differences between the ^{13}C resonances (Table VIII) due to C15 and C16 (the trans to O outside and inside entries) are greater in the hp complex (4.32 ppm) than in the mhp complex (0.88 ppm), again with the 2hq and chp complexes giving intermediate values (2.69 and 2.00, respectively). In this case, the trend is the opposite of that observed for the proton resonances.

Similar effects are also seen in the chemical shifts between the resonances due to H11 and H12 and C11 and C12. These shifts probably have a significant steric genesis due to interactions between H11 on one COD ligand and H11, H16, and H17 on the other COD ligand. Here the differences in the ^{13}C signals are much larger than those of the ^{1}H signals.

The second source of geometric chemical shift differences between "inside" and "outside" atom pairs is magnetic anisotropy. In the $[M(COD)(\mu\text{-}L)]_2$ complexes, we can identify four sources of anisotropy: the metal–metal interaction, electronic circulation in π-symmetry orbitals of the distal metal, the aromatic ring currents of the pyridine rings, and the carbon–carbon double bonds of the COD ligands. In principle, a McConnell treatment[38] (similar to that used by McGlinchey for M≡M triple bonds)[39] that takes into account the distance and angle between the atoms in question and the center of each source of anisotropy could be used to calculate the magnetic anisotropy of the M–M interaction, but in practice, such a calculation would be quite tedious. At first glance, an attractive simplification would ascribe the magnetic anisotropy solely to the geometric orientation of nuclei relative to the d^8–d^8 interaction, but upon further analysis, we believe this to be a minor source of anisotropy. First, the d^8–d^8 interaction is in essence a σ interaction and no substantial electronic circulation in the plane normal to the bond vector is expected. Additionally, because magnetic anisotropy is independent of the particular nucleus under observation,[39] a similar chemical shift difference should be generated between H inside/outside pairs (H11 and H12 for example) and the same C inside/outside pair (C11 and C12) because they have similar geometric factors relative to the center of the metal–metal interaction and the distal metal. Experimentally, the proton shift difference in $[Ir(COD)(\mu\text{-hp})]_2$ for this case of 0.56 ppm is much smaller than the carbon chemical shift difference (15.2 ppm). Magnetic anisotropy from the d^8–d^8 M–M interaction or the distal metal is probably unimportant in these systems.

The aromatic ring current of the hydroxypyridine ligands and the circulation of electron density around the carbon–carbon double bonds of the COD ligands are more likely responsible for that portion of the chemical shift difference in the signals of the olefinic atoms not due to steric effects. For example, H15 (trans to O and outside) is close to the pyridine ring, H16 (trans to O and inside) is close to both carbons of the C11–C12 double bond, H11 (trans to N and inside) is tucked into the area between the inside carbons (C11 and C16) of the two double bonds of the opposing COD ligand, and H12 is not particularly close to any major source of anisotropy. Thus, each olefinic proton has a specific relationship to well-known anisotropy sources. This hypothesis is also consistent with the ^{13}C resonances, particularly for C12, which has the most extreme chemical shift of the four olefinic carbons and again is the farthest away from any source of magnetic anisotropy.

Conclusions

The new compounds of the form $[M(COD)(\mu\text{-}L)]_2$ have been characterized by X-ray crystallography as binuclear complexes with twisted, open-book structures. The solution- and gas-phase structures of the compounds are quite similar. The ^{1}H NMR spectra of all the compounds were completely assigned through the application of 2D and NOE techniques. The chemical shift differences between "inside" and "outside" but otherwise equivalent ^{1}H and ^{13}C nuclei pairs are ascribed to sterically generated hybridization differences and magnetic anisotropy generated by the orientations of the pyridine rings and the COD carbon–carbon double bonds. Our data suggest that the magnetic anisotropy of the d^8–d^8 interaction is small.

Acknowledgment. We wish to thank Professor J. D. Britton for his expert assistance in the X-ray structure determinations and Johnson-Matthey for loans of rhodium and iridium trichlorides. The X-ray diffractometer was purchased in part through funds provided by National Science Foundation Grant CHE77-28505.

Registry No. $[Ir(COD)(\mu\text{-hp})]_2$, 98330-72-4; $[Ir(COD)(\mu\text{-mhp})]_2$, 98330-73-5; $[Ir(COD)(\mu\text{-chp})]_2$, 115677-35-5; $[Ir(COD)(\mu\text{-2hq})]_2$, 115677-36-6; Ir(COD)(8hq), 76770-89-3; $[Rh(COD)(\mu\text{-hp})]_2$, 112021-29-1; $[Rh(COD)(\mu\text{-mhp})]_2$, 115677-37-7; Rh(COD)(8hq), 33409-86-8; $[Ir(COD)(\mu\text{-Cl})]_2$, 12112-67-3; Na(hp), 930-70-1; Na(mhp), 13472-90-7; Na(chp), 59432-71-2; Na(2hq), 5852-89-1; Na(8hq), 2872-54-0; $[Rh(COD)(\mu\text{-Cl})]_2$, 12092-47-6; $[Rh(COD)(CH_3CN)_2][BF_4]$, 32679-02-0.

Supplementary Material Available: Listings of hydrogen atom parameters (Tables S1 and S3), anisotropic thermal parameters (Tables S2 and S4), bond distances (Tables S7 and S8), bond angles (Tables S9 and S10), and least-squares planes (Tables S11 and S12) for $[Ir(COD)(\mu\text{-mhp})]_2$ and $[Rh(COD)(\mu\text{-mhp})]_2$, dihedral angles for $[M(COD)(\mu\text{-mhp})]_2$ (Table S13), IR spectral data for the synthesized complexes (Table S14), and calculated and observed allylic coupling constants for $[Ir(COD)(\mu\text{-hp})]_2$ and relevant dihedral angles (Table S15) and figures showing the ORTEP structure of $[Rh(COD)(\mu\text{-mhp})]_2$ (Figure S1), simulated and experimental ^{1}H NMR spectra of the COD region of $[Ir(COD)(\mu\text{-hp})]_2$ (Figure S2), and COSY spectrum of the COD region of $[Ir(COD)(\mu\text{-mhp})]_2$ (Figure S3) (23 pages); listings of calculated and observed structure factors for $[Ir(COD)(\mu\text{-mhp})]_2$ and $[Rh(COD)(\mu\text{-mhp})]_2$ (Tables S5 and S6) (30 pages). Ordering information is given on any current masthead page.

(37) (a) Platzer, N.; Goasdove, N.; Bonnaire, R. J. *J. Organomet. Chem.* **1978**, *160*, 455. (b) Bonnaire, R.; Manoli, J. M.; Potvin, C.; Platzer, N.; Goasdove, N. *Inorg. Chem.* **1981**, *20*, 2691.
(38) McConnell, H. M. *J. Chem. Phys.* **1957**, *27*, 226.
(39) (a) McGlinchey, M. J. *Inorg. Chem.* **1980**, *19*, 1392. (b) McGlinchey, M. J.; Burns, R. C.; Hofer, R.; Top, S.; Jaoven, G. *Organometallics* **1986**, *5*, 104.